

# Climate change in India inferred from geothermal observations

Sukanta Roy,<sup>1</sup> Robert N. Harris,<sup>2</sup> R. U. M. Rao,<sup>1</sup> and David S. Chapman<sup>2</sup>

Received 1 May 2001; revised 10 August 2001; accepted 19 August 2001; published 20 July 2002.

[1] Temporal variations in surface ground temperature impart a signal to the subsurface thermal regime that is captured in borehole temperature-depth profiles. Seventy temperature-depth profiles in India, located between 12° and 28°N, are analyzed to infer past changes in ground temperature. These profiles exhibit predominantly positive anomalous temperatures relative to the background thermal regime beginning at depths of 75–150 m and increasing toward the surface. This pattern is consistent with warming over the past century. An interpretation in terms of linear surface temperature change indicates warming of about  $0.9^\circ \pm 0.1^\circ\text{C}$  over the past 150 years. Relatively complete surface air temperature (SAT) records from meteorological stations near the boreholes indicate similar rates of warming over the last century. A combined analysis of borehole temperatures and SAT records yields a long-term, preobservational mean temperature,  $0.8^\circ \pm 0.1^\circ\text{C}$  lower than the 1961–1990 mean SAT. When the most recent decade is included directly in the analysis, the average total warming in India from the early 1800s to the late 1990s is  $\sim 1.2^\circ\text{C}$ . **INDEX TERMS:** 1645 Global Change: Solid Earth; 1694 Global Change: Instruments and techniques; 3329 Meteorology and Atmospheric Dynamics: Mesoscale meteorology; 3309 Meteorology and Atmospheric Dynamics: Climatology (1620); **KEYWORDS:** India, climate change, borehole temperatures, global warming

## 1. Introduction

[2] The impacts of climate change represent an additional stress in developing countries that are already facing pressures due to rapid urbanization, industrialization, and economic development. India is especially vulnerable to the impacts of climate change because of its large and growing population, a densely populated and low-lying coastline, and an economy that is closely tied to its natural resource base. Because climate records within India are generally only available over the past century or so, it is particularly important to exploit measures of climate change that can extend these records back in time. One such measure can be found in subsurface temperature-depth profiles.

[3] Variations in surface ground temperature (SGT) at the Earth's surface diffuse downward in a predictable way causing systematic perturbations to the subsurface temperature field. The magnitude and depth extent of these perturbations provide a direct measure of the magnitude and timing of temperature changes at the surface [Beck and Judge, 1969; Lachenbruch and Marshall, 1986; Lachenbruch et al., 1988; Chapman et al., 1992; Mareschal and Beltrami, 1992; Wang, 1992; Cermak et al., 1992; Beltrami and Chapman, 1994; Deming, 1995; Harris and Chapman, 1997, 1998a, 1998b; Pollack et al., 1998; Guillou-Frottier et al., 1998; Harris and Gosnold, 1999; Huang et al., 2000]. The depth extent of these anomalies is governed

by the rock material property thermal diffusivity such that subsurface temperatures in the top 200 m potentially contain a record of SGT variations over approximately the past 300 years. Because heat transfer is a diffusive process, Earth acts as a low-pass filter for surface temperature changes. High-frequency components are attenuated, but important decadal and century SGT trends through time can be confidently resolved.

[4] Geothermal observations and analyses contribute to climate change studies in several ways. First, geothermal observations can extend our knowledge of surface temperature variations both spatially and temporally. Globally, very few surface air temperature (SAT) records exist prior to 1860, and those that do are mostly limited to Europe and eastern North America [Hansen and Lebedeff, 1987]. For example, in India, SAT records are only extensively available starting about 1901 [Rupa Kumar et al., 1994]. Second, if borehole temperature perturbations are correlated with SAT time series, then temperature-depth profiles have the potential of filling gaps in the SAT record of climate change and extending records of surface temperature change back in time. In this sense, borehole data may be an important complement to SAT records. Third, borehole data can be used to address whether current global warming trends inferred from SAT data [Hansen and Lebedeff, 1987; Jones et al., 1999] result from data coverage starting near a climatic temperature minimum in the late 1800s or whether they represent significant long-term climate change [Ellsaesser et al., 1986]. In this regard, multicentury proxy reconstructions [Overpeck et al., 1997; Jones et al., 1998; Mann et al., 1998, 1999; Crowley and Lowery, 2000] have been useful in showing that the past 100 years of warming has been anomalous. However, in

<sup>1</sup>National Geophysical Research Institute, Hyderabad, India.

<sup>2</sup>Department of Geology and Geophysics, University of Utah, Salt Lake City, Utah, USA.

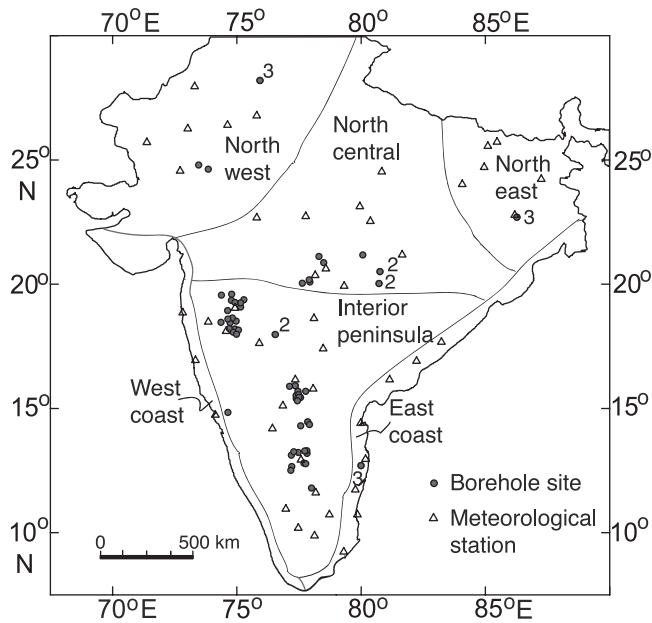


**Figure 1.** Indian peninsula showing locations of the 70 boreholes (solid circles) and 48 meteorological stations (open triangles) used in this study. Multiple boreholes at the same site are indicated by numbers. The six climatic provinces adopted from *Hingane et al.* [1985] are also shown.

contrast to proxy records, which have to be transformed to temperature through a calibration process, borehole temperature profiles constitute a direct measure of temperature variation.

[5] This paper analyzes temperature-depth records obtained from 70 boreholes distributed over a number of climatic provinces in India (Figure 1) for evidence of past SGT variations. Importantly, these boreholes constitute an extensive data set for the low latitude regions  $\sim 12\text{--}28^\circ\text{N}$ , a latitude band that is underrepresented in geothermal climate change studies. After reviewing climate change results based on SAT records we analyze the borehole data and then combine these results with a simple analysis of SAT data to check for consistency and to investigate trends prior to the widespread recording of SAT data.

## 2. Surface Air Temperature Data

[6] Surface air temperature (SAT) records obtained from meteorological stations constitute one of the key indicators of climate change. It is instructive to review warming trends in India determined from SAT data alone and then to compare these trends with results of analyzing borehole temperature profiles. A number of studies have investigated long-term trends in SAT data over the Indian landmass [Pramanik and Jagannathan, 1954; Jagannathan and Parthasarathy, 1972; Hingane et al., 1985; Sarker and Thapliyal, 1988; Thapliyal, 1990; Thapliyal and Kulshrestha, 1991; Srivastava et al., 1992; Rupa Kumar et al., 1994]. India consists of six major climatic provinces based on relatively uniform geographical, topographical, and climatological features (Figure 1). These provinces are the north-

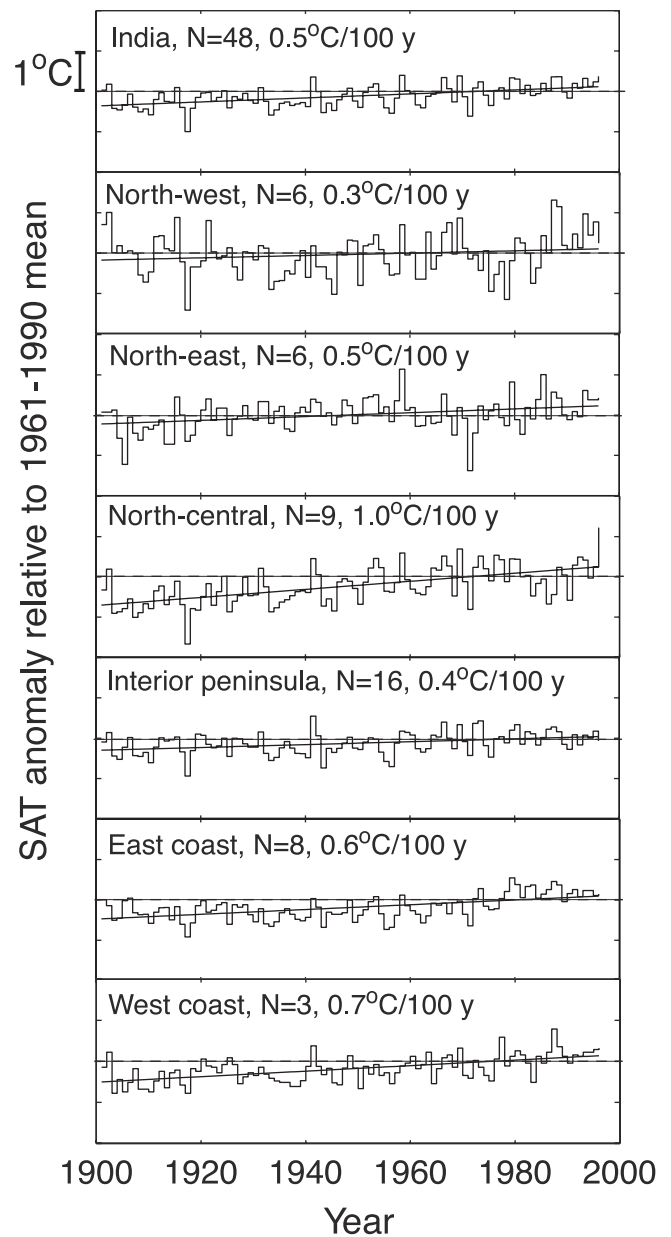


**Figure 2.** SAT time series for climatic provinces in India. The SAT data are shown as annual departures from the 1961–1990 mean temperature (dashed line). Solid line shows best linear fit to the data. The number of stations and average rates of increase of SAT (in  $^\circ\text{C}/100$  years) are indicated.

**Table 1.** Average SAT Trends for the Different Climatic Provinces

Climatic Division	Number of Stations	Average Trend, $^\circ\text{C}/100$ years
Northwest (NW)	6	0.3
North central (NC)	9	1.0
Northeast (NE)	6	0.5
East coast (EC)	8	0.6
West coast (WC)	3	0.7
Interior peninsula (IP)	16	0.4
All sites	48	0.5

**Table 2.** Analysis of Temperature-Depth Profiles and Results of Ramp Inversion for SGT Change<sup>a</sup>

Location, Borehole	Long. °E	Lat. °N	Year of T-z Log	Ramp Inversion						Data Ref. <sup>c</sup>	
				Depth Interval, <sup>b</sup> m	g, mK m <sup>-1</sup>	T <sub>0</sub> , °C	ΔT, °C	t*, years	RMS, mK		Onset Year
Northwest (NW) Province											
Khetri, S-47	75.93	28.20	1965	180–700	21.6	28.6	0.7	129	57	1836	1
Khetri, S-48	75.93	28.20	1965	178–456	21.4	28.1	2.3	189	56	1776	1
Khetri, S-49	75.93	28.20	1965	178–485	20.3	28.4	1.1	108	43	1857	1
Jaswantgarh, J	73.46	24.80	1994	111–150	15.9	25.7	0.8	41	14	1953	5
Merta, M	73.85	24.63	1994	111–156	13.9	28.0	−0.1	58	14	1936	5
North Central (NC) Province											
Mogarra, MGA-18	80.07	21.18	1985	183–260	12.8	28.7	2.6	112	39	1873	4
Palora, W-3	78.30	21.12	1994	111–195	36.2	27.6	3.5	51	69	1943	5
Mandwa, W-1	78.49	20.87	1994	111–204	28.0	26.7	3.8	64	109	1930	5
Bodal, BDL-168	80.76	20.51	1985	188–530	24.6	25.5	2.1	274	43	1711	4
Bodal, BDL-169	80.76	20.51	1985	183–659	23.8	25.6	2.5	283	55	1702	4
Loni, Y-7	77.91	20.18	1994	111–162	35.3	28.8	−0.4	87	62	1907	5
Dattarampur, Y-4	77.94	20.09	1994	111–189	36.3	28.8	1.8	27	131	1967	5
Singad, Y-3	77.63	20.04	1994	111–147	28.9	28.3	3.1	45	42	1949	5
Malanjkhanda, MDN-4	80.72	20.03	1985	183–433	15.3	25.2	1.6	295	41	1690	4
Malanjkhanda, MDN-7	80.72	20.03	1985	181–440	15.2	26.0	−0.3	240	29	1745	4
Northeast (NE) Province											
Narwapahar, NRW-92	86.27	22.70	1968	179–460	16.4	27.5	2.4	160	36	1808	2
Narwapahar, NRW-125	86.27	22.70	1968	180–460	18.1	26.7	2.3	234	36	1734	2
Narwapahar, NRW-127	86.27	22.70	1968	186–317	17.6	26.9	−0.6	116	42	1852	2
Interior Peninsula (IP)											
Taklibhan, AN-8	74.79	19.60	1994	111–201	18.4	28.8	1.8	58	27	1936	5
Nimgaojali, AN-11	74.38	19.56	1994	111–198	44.9	27.2	3.3	50	43	1944	5
Ghotan, AN-6	75.28	19.38	1994	111–189	20.2	28.7	2.6	57	15	1937	5
Brahmani, AN-16	74.78	19.35	1994	111–189	18.7	30.4	2.4	55	18	1939	5
Singva Keshav, AN-17	74.92	19.27	1994	111–171	24.8	28.0	0.7	45	11	1949	5
Padli, AN-7	75.15	19.25	1994	111–183	23.1	27.8	1.4	60	12	1934	5
Manikdaundi, AN-5	75.15	19.08	1994	111–184	24.4	27.1	1.0	40	29	1954	5
Astagaon, AN-19	74.63	18.94	1994	111–180	22.8	26.7	0.9	57	15	1937	5
Matar Pimpri, AN-4	74.64	18.60	1994	111–180	26.4	28.6	0.2	73	35	1921	5
Torkurwadi, AN-1	74.97	18.52	1994	111–183	23.0	29.4	0.01	9	13	1985	5
Ambegaon, PU-2	74.36	18.47	1995	111–198	17.6	30.5	1.1	38	16	1957	5
Sidhatek, AN-2	74.73	18.45	1994	111–201	23.5	27.6	1.6	80	15	1914	5
Nirgude, PU-5	74.70	18.22	1995	111–200	23.7	28.5	0.1	136	29	1859	5
Loni Deokar, PU-1	74.92	18.20	1994	111–195	19.6	29.0	1.5	68	21	1926	5
Malwadi, PU-7	75.06	18.16	1995	111–180	23.1	28.5	1.9	66	24	1929	5
Gotoundi, PU-6	74.86	18.07	1995	111–196	26.9	28.3	−1.2	34	15	1961	5
Vakilbasthi, PU-8	74.99	17.99	1995	111–186	22.2	27.7	2.1	12	29	1983	5
Hulli, KIL-26	76.53	17.98	1995	111–183	23.4	27.1	2.4	53	56	1942	5
Petsangvi, KIL-27	76.55	17.98	1995	111–174	19.9	28.2	2.4	64	24	1931	5
Ratsamarri, K-5	77.35	15.91	1994	111–192	7.9	30.8	1.1	58	8	1936	5
Ratsamarri, K-6	77.35	15.91	1994	111–195	8.0	30.8	0.7	67	6	1927	5
Halvi, K-4	77.12	15.89	1994	111–186	11.7	30.3	0.6	52	6	1942	5
Kodumuru, K-1	77.77	15.69	1994	111–195	10.7	30.5	0.4	66	19	1928	5
Kandanati, K-2	77.46	15.69	1994	111–195	10.7	30.6	0.4	74	29	1920	5
Khairupla, K-13	77.48	15.56	1994	111–198	15.9	29.4	0.9	14	11	1980	5
Johrapuram, K-7	77.39	15.40	1994	111–195	9.0	28.1	1.2	62	43	1932	5
Hosur Road, K-8	77.46	15.38	1994	111–201	13.4	30.0	0.3	42	11	1952	5
Haligeri, K-11	77.39	15.52	1994	111–177	14.3	29.9	0.9	25	10	1969	5
Haligeri, K-12	77.39	15.52	1994	111–165	13.8	29.9	0.2	73	10	1921	5
Dudekonda, K-16	77.50	15.45	1994	111–195	14.6	29.7	0.6	23	9	1971	5
Dudekonda, K-17	77.50	15.45	1994	111–180	14.8	29.7	0.8	9	11	1985	5
Dudekonda, K-15	77.56	15.44	1994	111–186	13.4	29.8	0.9	46	21	1948	5
Burzula, K-18	77.44	15.31	1994	111–195	7.8	28.2	1.5	59	42	1935	5
Arbail, ARB-61	74.64	14.84	1988	180–557	15.9	24.7	1.7	35	39	1953	6
Kanamukala, KA-I	77.57	14.30	1987	111–198	11.0	29.9	2.0	46	8	1941	3
Upparalapalli, UP-1	77.85	14.46	1987	111–198	11.7	30.3	−0.06	26	13	1961	3
Upparalapalli, UP-2	77.85	14.46	1987	111–200	11.8	30.1	0.8	60	46	1927	3
A.B. Palli, D-15	77.92	14.35	1987	111–177	14.5	30.5	2.4	4	20	1983	6
Vijayapura, B-7	77.81	13.30	1994	180–267	10.5	26.9	0.7	132	16	1862	5
L.G. Halli, B-8	77.73	13.29	1994	180–243	10.3	27.0	0.7	7	16	1987	5
Manne, B-17	77.29	13.26	1994	180–255	11.9	25.6	1.5	108	13	1886	5
Mellohalli, B-10	77.47	13.23	1994	110–195	7.2	27.7	0.7	56	11	1938	5
Sulebele, B-6	77.82	13.19	1994	180–246	7.4	27.1	1.1	145	45	1849	5
Malligunte, B-16	77.19	13.12	1994	180–291	6.8	26.8	1.0	166	32	1828	5
Chandapur, B-1	77.70	12.80	1994	111–207	7.2	26.6	0.8	76	33	1918	5

**Table 2.** Analysis of Temperature-Depth Profiles and Results of Ramp Inversion for SGT Change<sup>a</sup>

Location, Borehole	Long. °E	Lat. °N	Year of $T$ - $z$ Log	Ramp Inversion						Data Ref. <sup>c</sup>	
				Depth Interval, <sup>b</sup> m	$g$ , mK m <sup>-1</sup>	$T_0$ , °C	$\Delta T$ , °C	$t^*$ , years	RMS, mK		Onset Year
Attibele, B-2	77.77	12.78	1994	180–247	8.0	26.8	1.4	111	22	1883	5
Chennapatna, B-12	77.21	12.66	1994	111–219	4.4	28.5	1.5	67	46	1927	5
Nunnur, B-13	77.17	12.51	1994	111–201	4.2	29.2	0.8	65	35	1929	5
Elur	78.11	11.34	1997	180–300	19.3	30.1	3.6	90	23	1907	6
<i>East Coast (EC) Province</i>											
KPK-1	79.9	12.59	1996	180–595	13.8	30.2	0.8	394	38	1602	6
KPK-2	79.9	12.59	1996	180–618	13.5	30.2	1.9	294	36	1702	6
KPK-3	79.9	12.59	1996	180–575	13.6	30.1	2.2	239	28	1757	6

<sup>a</sup>g, gradient; T<sub>0</sub>, zero-depth (surface) intercept of linear fit; ΔT, magnitude of ramp change of surface temperature over a duration t\*; RMS, root-mean-square misfit between reduced temperature profile and ramp fit.

<sup>b</sup>Depth section of T-z profile used for computation of background temperature gradient.

<sup>c</sup>References: 1, Gupta *et al.* [1967]; 2, Rao and Rao [1974]; 3, Gupta *et al.* [1991]; 4, Gupta *et al.* [1993]; 5, Roy and Rao [2000]; 6, unpublished data.

west (NW), north central (NC), northeast (NE), west coast (WC), interior peninsula (IP), and east coast (EC).

[7] Hingane *et al.* [1985] found that 30 of 73 meteorological stations investigated showed a significant warming trend, while six stations show a significant cooling trend. At the province scale, significant warming trends were found in the WC, IP, NC, and NE provinces. Overall, the mean annual SAT data indicate a warming trend of 0.4°C over the past 100 years significant at the 99% level. More recently, Rupa Kumar *et al.* [1994], using 121 stations with data between 1901 and 1987, analyzed maximum and minimum temperature trends and found that while mean maximum temperatures have risen 0.6°C/100 years, significant at the 99% confidence level, minimum temperatures have not significantly warmed (0.1°C/100 years). Further, they conclude that the mean warming trends in India are due to increasing maximum temperatures. A third finding is that differences in warming trends between urban and nonurban stations are not significant [Rupa Kumar and Hingane, 1988; Rupa Kumar *et al.*, 1994]. These results are somewhat at odds with SAT data in rest of the Northern Hemisphere which indicate that minimum temperatures are increasing and that there is a significant difference in warming trends between urban and nonurban areas.

[8] To make comparisons between SAT data and our borehole analysis, we have compiled 48 meteorological stations that are in relatively close proximity to our borehole sites (Figure 1). The meteorological data are drawn from the India Meteorological Department (IMD) and are relatively complete over the time range 1901–1996. In anticipation of ultimately comparing the SAT data to the borehole analysis, we group the meteorological data by province. Within each province individual mean annual SAT time series are referenced to the 1961–1990 interval and averaged (Figure 2). Trends for each province are estimated by linear regression and reported as a trend per 100 years (Table 1). For the whole of India, the IP and the NE provinces, our trends are similar to those reported by Hingane *et al.* [1985] and Rupa Kumar *et al.* [1994]. However, trends for the NW, NC, and EC provinces are slightly higher than those previously reported. These discrepancies likely arise because we use fewer stations than those used in previous studies, in association with our

requirement of proximity between borehole sites and meteorological stations.

### 3. Borehole Temperature-Depth Data

[9] Borehole temperature data from many sites in the Indian shield have been acquired over the last three and half decades for evaluation of terrestrial heat flow [see Gupta, 1995; Roy and Rao, 2000, and references therein]. The boreholes were drilled for mineral exploration and groundwater exploitation in both Precambrian crystalline terrains and sedimentary basins. Boreholes drilled for mineral exploration are diamond drilled, and temperatures within them generally recover up to 95% of their undisturbed values within 48 hours after completion of drilling [Jaeger, 1961; Roy and Rao, 1999, 2000]. Boreholes drilled for groundwater resources are percussion drilled. In many of these boreholes, groundwater yields were poor, and the wells were either abandoned or unused for at least 6 months and up to 2 years prior to logging. Thus temperature measurements made in both sets of boreholes are not likely to be disturbed by drilling. The measurements were made by manually lowering a calibrated Fenwal thermistor probe and measuring the transducer resistance to a precision of 0.1 Ω using a Wheatstone bridge. Our temperature precision with this equipment is ±3 mK for a 1 kΩ thermistor [Roy and Rao, 2000]. In practice, because temperature measurements in boreholes are affected by borehole thermal stability and instrumental noise and stability, temperatures are generally reproducible to better than 20 mK, as indicated by comparisons of multiple temperature logs.

[10] Boreholes drilled for purposes such as mineral exploration or groundwater potential are often not optimally located for climate change studies. Temperatures measured in such boreholes may be influenced by one or more of the following effects: (1) systematic thermal conductivity variations in the rock penetrated by and surrounding a borehole, (2) topographic relief, (3) changes in surface vegetation in space and time, and (4) movement of groundwater at shallow depths. Such perturbations potentially simulate, degrade, or destroy climate change related thermal signatures [Roy *et al.*, 1972; Blackwell *et al.*, 1980; Lachenbruch and Marshall, 1986; Chisholm and Chapman, 1992; Lewis and Wang, 1992; Harris and Chapman, 1995; Guillou-Frottier *et al.*,

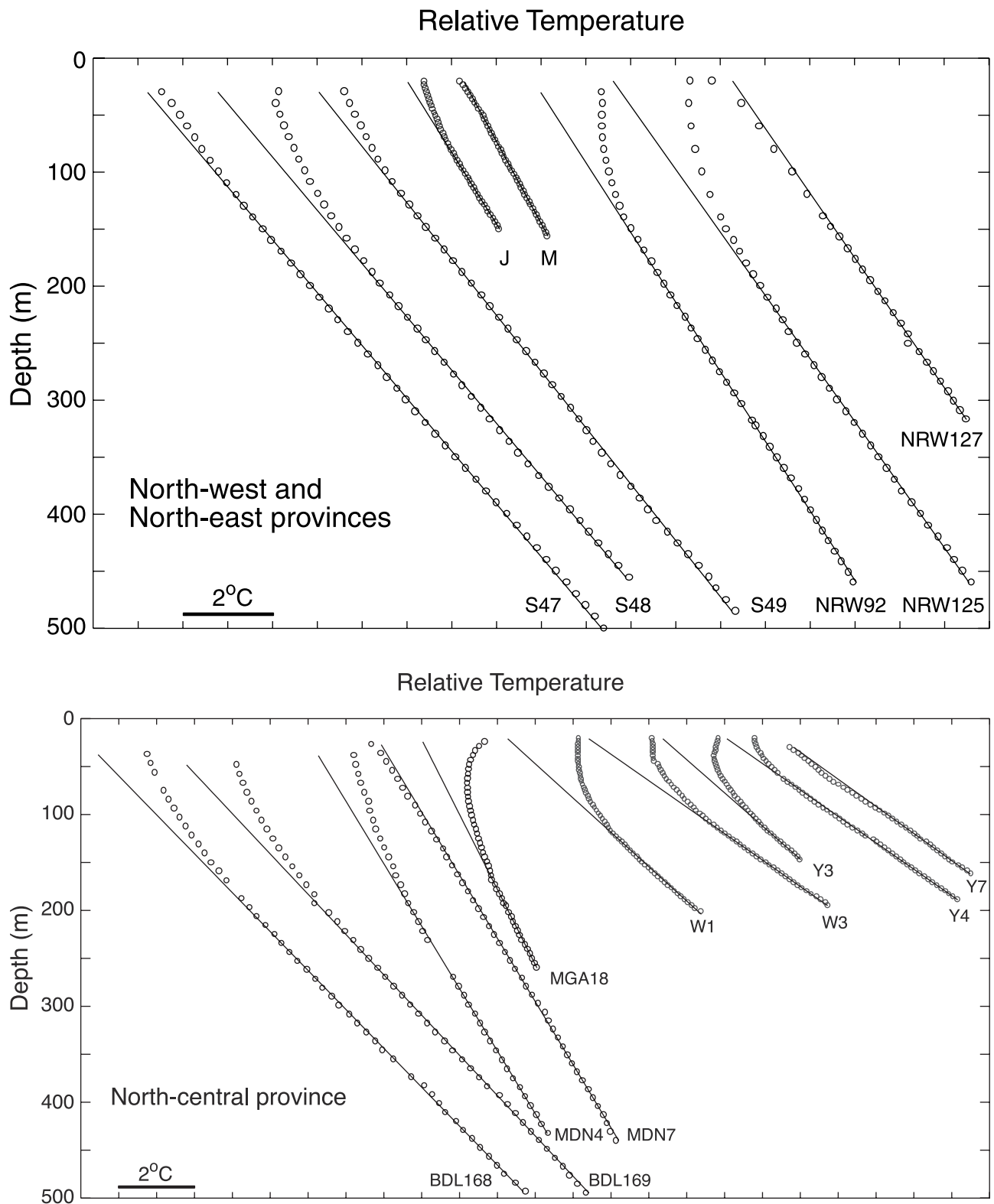


**Figure 3.** Plots of temperature-depth data (open circles) obtained at 70 carefully selected sites spatially distributed in the Indian peninsula. The background temperature profiles (solid lines) are obtained by fitting a line just below the curved upper portion in each  $T$ - $z$  profile. The boreholes are grouped according to climatic province (NW, NE, NC, IP, and EC); the identification numbers are indicated along each profile, and correspond to the boreholes listed in Table 2. Temperatures below 500 m are not displayed.



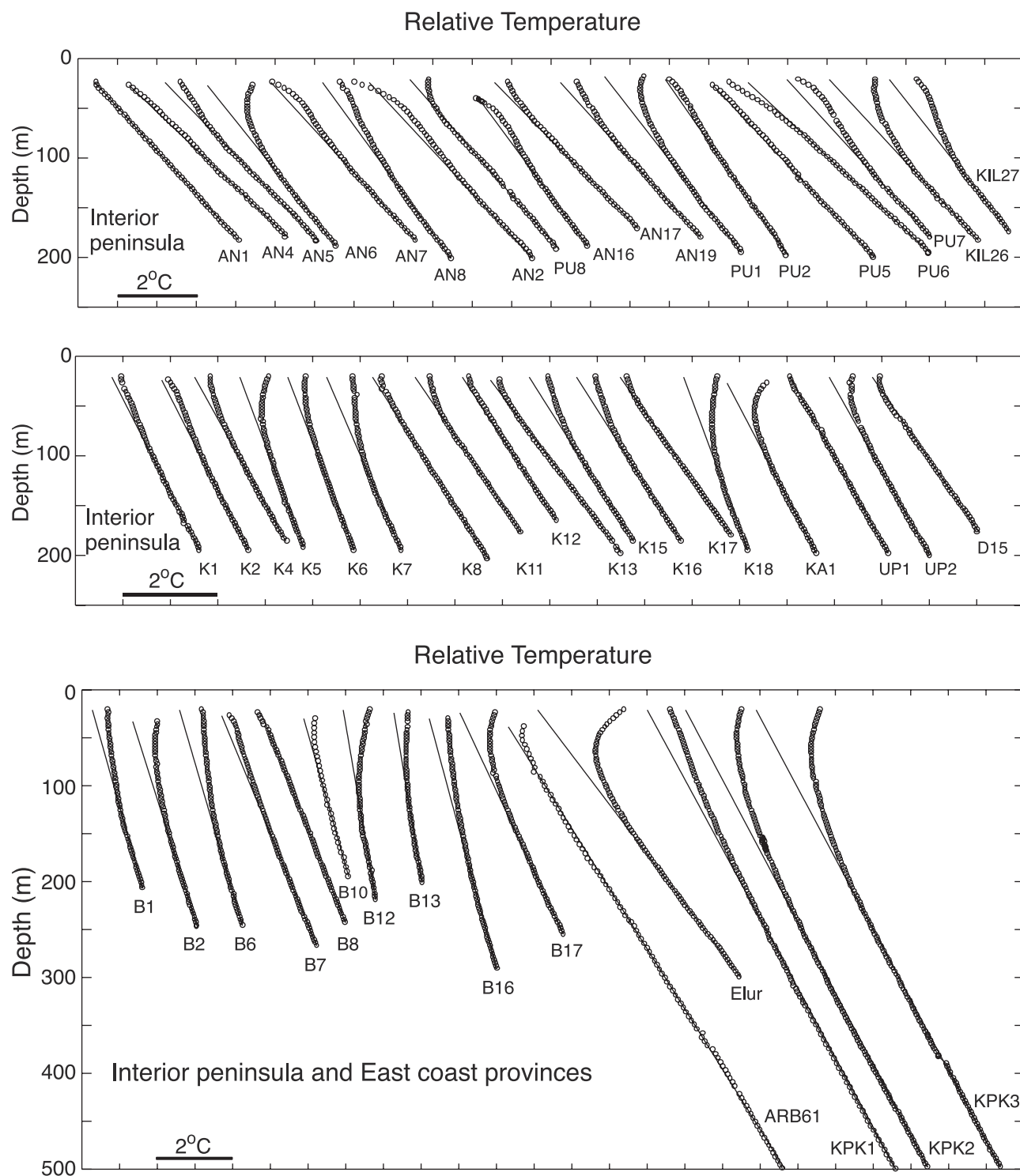
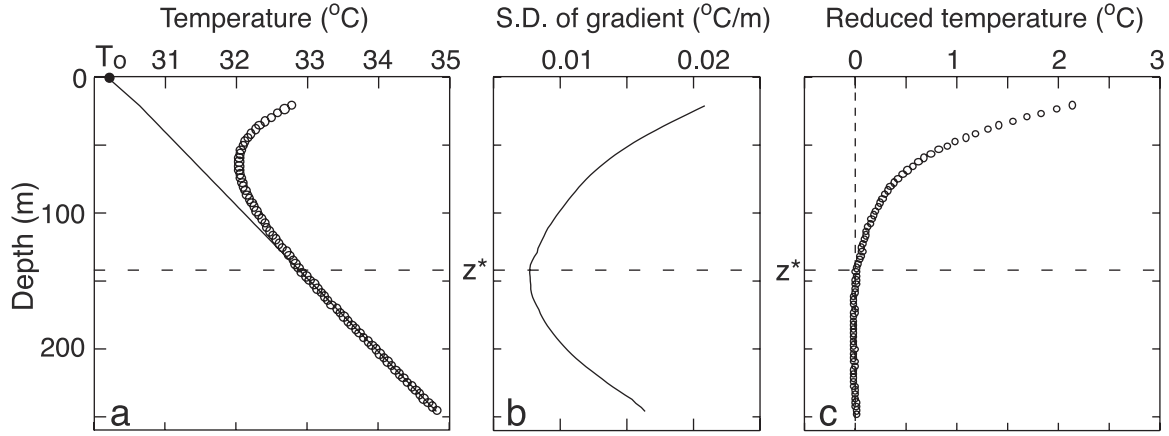


Figure 3. (continued)

1998]. To mitigate these factors, we screened the set of borehole data using the following criteria: (1) boreholes should intersect rocks with relatively uniform thermal conductivity to avoid misinterpreting temperature variations; (2) boreholes should be located in low-relief crystalline terrains to minimize topographic and fluid flow effects; and (3) temperature-depth profiles should have no visible features that are related to groundwater movement. An additional

requirement for geothermal climate change studies is the need to separate the background thermal regime from the climatically perturbed regime. Thus we also require temperature-depth logs to extend to at least 150 m. Of the available temperature-depth profiles, 172 were deeper than 150 m. Fifty-eight of these are from sedimentary basins and are discarded in the present study because of potentially large thermal conductivity variations and the increased potential



**Figure 4.** Illustration of the method for computing a reduced temperature profile for borehole Elur. (a) Temperature-depth measurements (open circles) and background thermal regime (solid line). (b) Standard deviation of thermal gradient as a function of the depth to start of linear fit ( $z^*$ ). The depth corresponding to the minimum indicates an optimum choice for  $z^*$ . (c) Reduced temperatures (open circles) are calculated by subtracting the background thermal regime from the measured temperatures. The dashed line corresponds to zero reduced temperature. The dashed horizontal lines in all three panels indicate the depth  $z^*$ .

for groundwater flow. These sorting criteria left 114 profiles from crystalline areas, and of these, 70 profiles were found to be in areas relatively unaffected by topographic and groundwater effects.

[11] Because the boreholes were not drilled primarily for climatic studies and because of the selection criteria, they are not evenly distributed across India (Figure 1). Nevertheless, the boreholes span five of the six major climatic provinces in India: NW, NC, NE, IP, and EC. The IP province contains the most boreholes, while the WC province does not contain any boreholes meeting our criteria. Borehole locations and other details for the 70 profiles selected for this study are given in Table 2.

[12] Temperature-depth profiles passing our screening process are displayed in Figures 3a–3e. Two patterns can be observed in most of these profiles. The deeper portion of each profile shows the expected increase in temperature with depth reflecting the conductive transfer of heat from the Earth's warm interior to the surface. Note that this portion is roughly linear, consistent with the assumptions of constant heat flow and uniform material properties at depth. At shallower levels, and superimposed on the regular increase in temperature with depth, are departures from linearity that are plausibly attributed to variations in SGT over time. These data show departures from linearity which begin at depths varying between about 150 and 75 m for individual profiles and increase toward the surface, supporting an interpretation of recent (order 100 years) and ongoing surface warming. Because SGT signals impart curvature to an otherwise linear increase in temperature with depth, it is possible to separate these signals.

#### 4. Analysis of Borehole Temperature-Depth Data

[13] The conductive temperature distribution in the Earth's subsurface is governed by the outward flow of heat from the Earth's interior and the temperature condition at the surface. The subsurface transient temperature perturba-

tion  $\Delta T(z, t)$  satisfies the one-dimensional heat diffusion equation,

$$\frac{\partial^2 \Delta T(z, t)}{\partial z^2} = \frac{1}{\alpha} \frac{\partial T}{\partial t}, \quad (1)$$

where the Earth's surface is at  $z = 0$ ,  $z$  is positive downward, and  $\alpha$  is the thermal diffusivity. With appropriate initial and boundary conditions, solutions to equation (1) provide a basis for interpreting curvature in the subsurface temperature field in terms of surface temperature variations.

[14] When thermal conductivities can be considered constant, a simple method for isolating temperature perturbations from the background thermal regime can be made by estimating the background thermal gradient based on a linear fit to the deeper portion of the data. Reduced temperatures  $T_R$  calculated in this manner are defined as [Chisholm and Chapman, 1992],

$$T_R(z) = T(z) - [T_0 + gz], \quad (2)$$

where  $T_0$  and  $g$  are a surface temperature intercept and thermal gradient, respectively. Because the thermal gradient and surface temperature intercept are estimated through a least squares fit to the data, these parameters are, to some extent, a function of the depth interval over which the data are fit. Our strategy for estimating the background thermal regime is illustrated in Figure 4 using temperature data from borehole Elur. To estimate the background thermal regime, we want to find a balance between using the deepest portion of the data where the climatic perturbation has the least influence and hence the background thermal regime is the best determined but using sufficient data to obtain a robust fit. We characterize this trade-off in terms of the standard deviation of the thermal gradient as a function of the depth to the start of the linear fit,  $z^*$ , and choose the depth which gives the minimum standard deviation. Because we are only removing a constant gradient from the temperature-depth

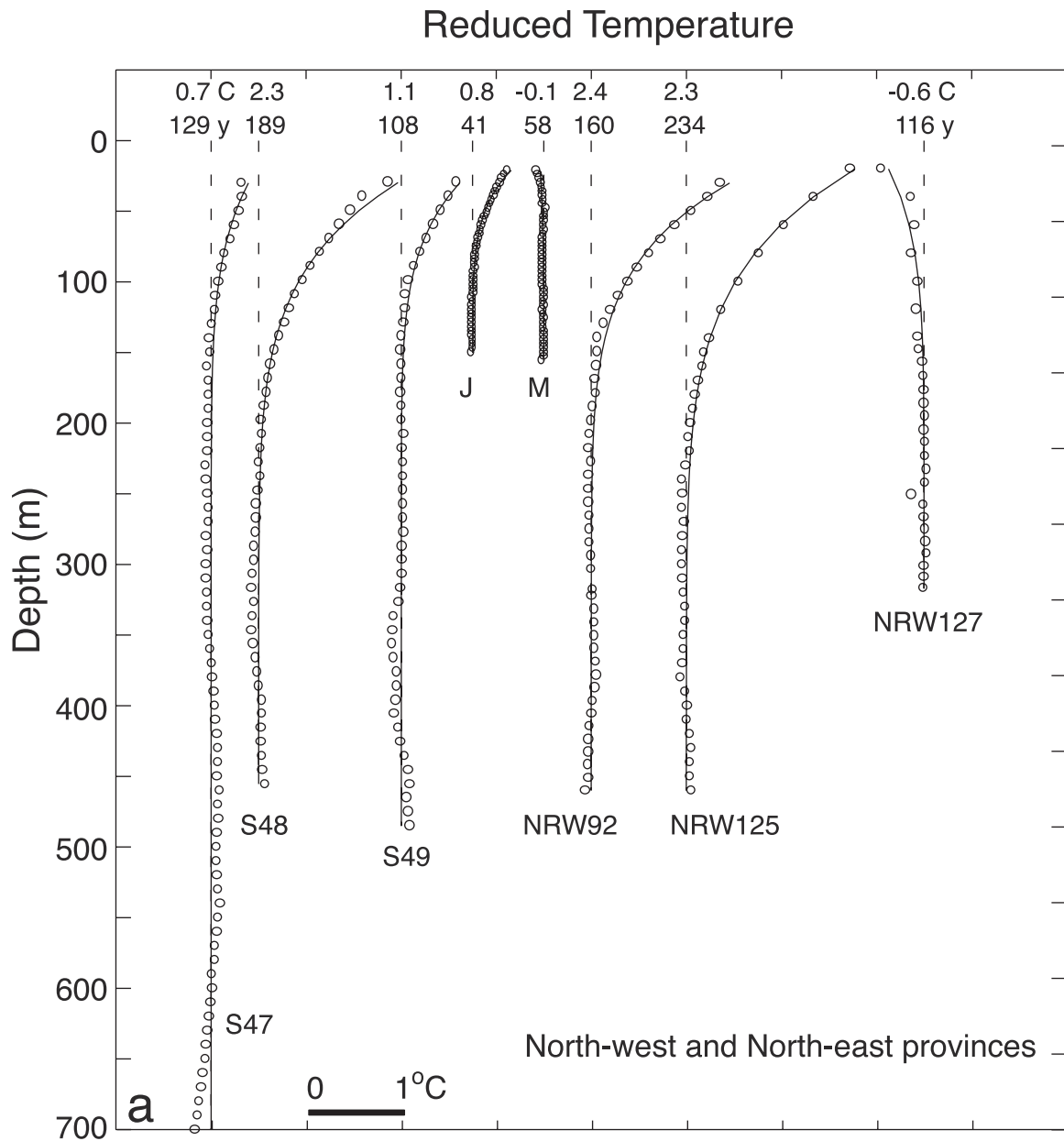


**Figure 5.** Reduced temperature profiles (open circles) for 70 boreholes used in this study. Each profile is offset to avoid overlap and plotted relative to zero reduced temperature (dashed line). Solid lines show the best fitting ramp models for the reduced temperature profiles corresponding to model parameters given in Table 2 and shown at the top of the profiles. In the case of eight profiles (AN2, AN7, AN8, AN16, PU2, PU7, KIL27, and B7) which show recent cooling above  $\sim 60$  m, ramps are fit below the depth of penetration of the most recent events.

profile and it is subsurface curvature that gets mapped into surface temperature variations according to equation (1), this step does not remove any climatic signal below  $z^*$ .

[15] An example of this technique is shown in Figure 4b. For example, the standard deviation of the gradient is large when the entire temperature profile is used because we are attempting to fit the curvature in the shallow subsurface. The standard deviation is also large when temperatures from only the deepest part of the hole are used because of the small number of measurement points. The depth corresponding to the minimum standard deviation indicates a suitable trade-off between these criteria. Because this process guarantees a

minimum misfit even in the case of boreholes unsuitable for climate analysis, additional criteria are sometimes used to restrict sites. As an example, in the case of borehole Elur, the minimum standard deviation,  $0.008^\circ\text{C}/\text{m}$ , is found using a depth of 141 m, although depths between 100 and 200 m yield similar results. The estimated background thermal regime using this technique is shown in Figure 4a, and the resulting reduced temperature profile for Elur is shown in Figure 4c.

[16] While not all temperature profiles indicate the same  $z^*$ , we found that using a starting depth of 180 m for boreholes deeper than 200 m and 110 m for boreholes



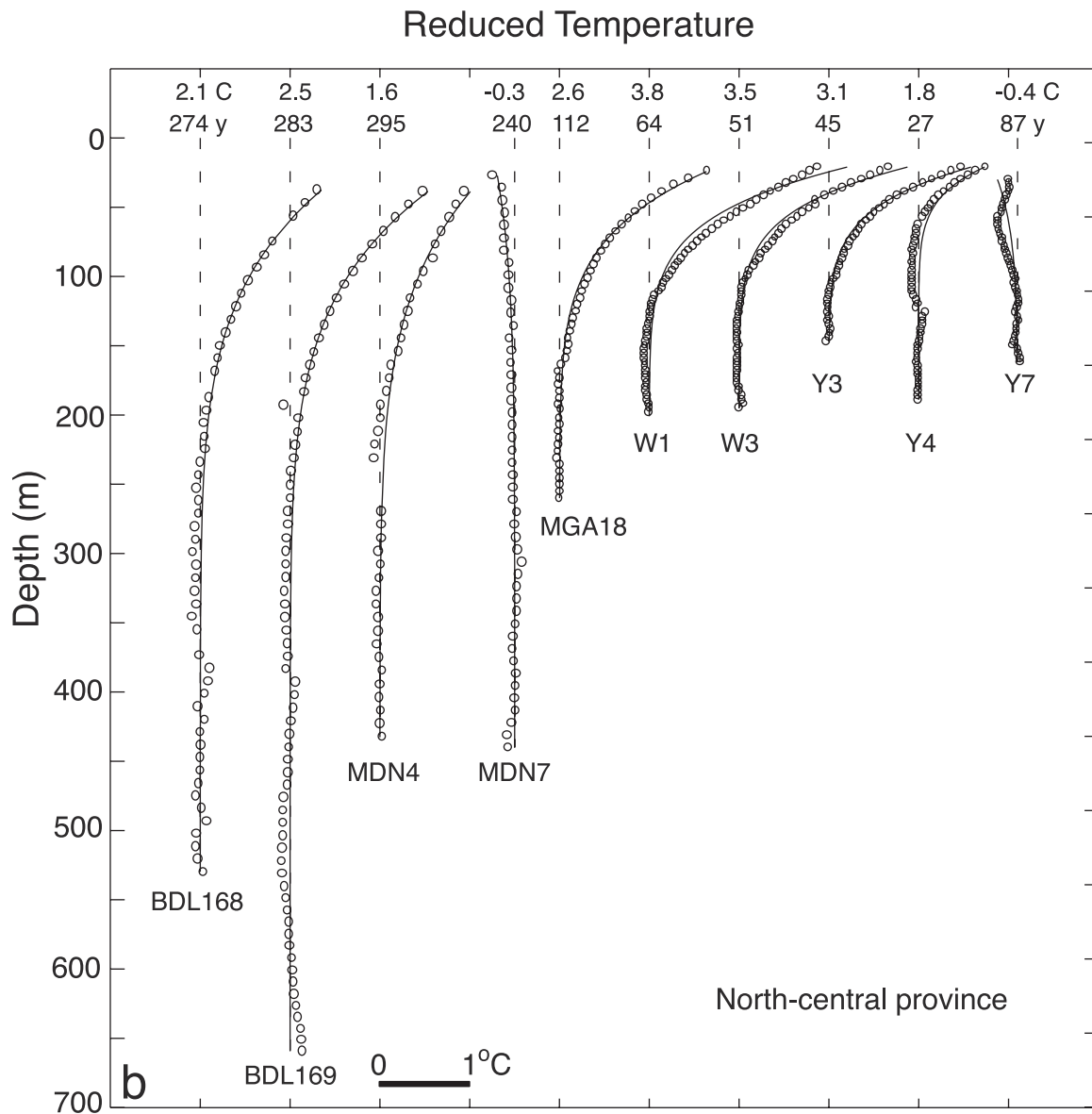


Figure 5. (continued)

shallower than 200 m is a reasonable choice. Choosing consistent values of  $z^*$  adds to the consistency of the analysis; it does not affect any curvature that might be manifested in the reduced temperature profiles. Estimated background thermal regimes for the rest of the boreholes are shown in Figure 3, and their parameters are given in Table 2. Surface temperature intercepts generally vary between 25 and 30°C and mostly follow a decreasing trend with increasing latitude. The background gradients generally range from 8 to 30 mK m<sup>-1</sup> consistent with published values of heat flow [Gupta *et al.*, 1967; Rao and Rao, 1974; Gupta *et al.*, 1991, 1993; Roy and Rao, 2000]. These additional checks add confidence to our background thermal regime estimates. Reduced temperature profiles (Figure 5) illustrate both the consistency and variability typically found in many continental areas [see, e.g., Harris and Chapman, 1995; Huang *et al.*, 2000]. For example, Figure 5a shows eight profiles for the NW and NE climatic provinces. Six of the eight profiles show positive temper-

ature excursions that begin at depths between 100 and 200 m and increase in amplitude toward the surface. Qualitatively, this pattern is consistent with recent and ongoing warming. However, two profiles show slight negative temperature excursions consistent with recent but modest cooling. In general, the reduced temperature profiles show predominantly positive temperature excursions beginning at depths of 75–150 m and which increase in amplitude toward the surface indicative of regional and persistent warming.

[17] To quantify estimates of recent ground warming, we invert the reduced temperature profiles for a SGT history. While many inversion techniques have been developed for this problem [Shen and Beck, 1991, 1992; Clow, 1992; Wang, 1992; Mareschal and Beltrami, 1992; Harris and Chapman, 1995; Huang *et al.*, 2000], we chose to model the reduced temperature profiles in terms of a linear change in surface temperature (a ramp) as did Lachenbruch and Marshall [1986] in their seminal study of boreholes in Alaska. This process emphasizes first-order variations in

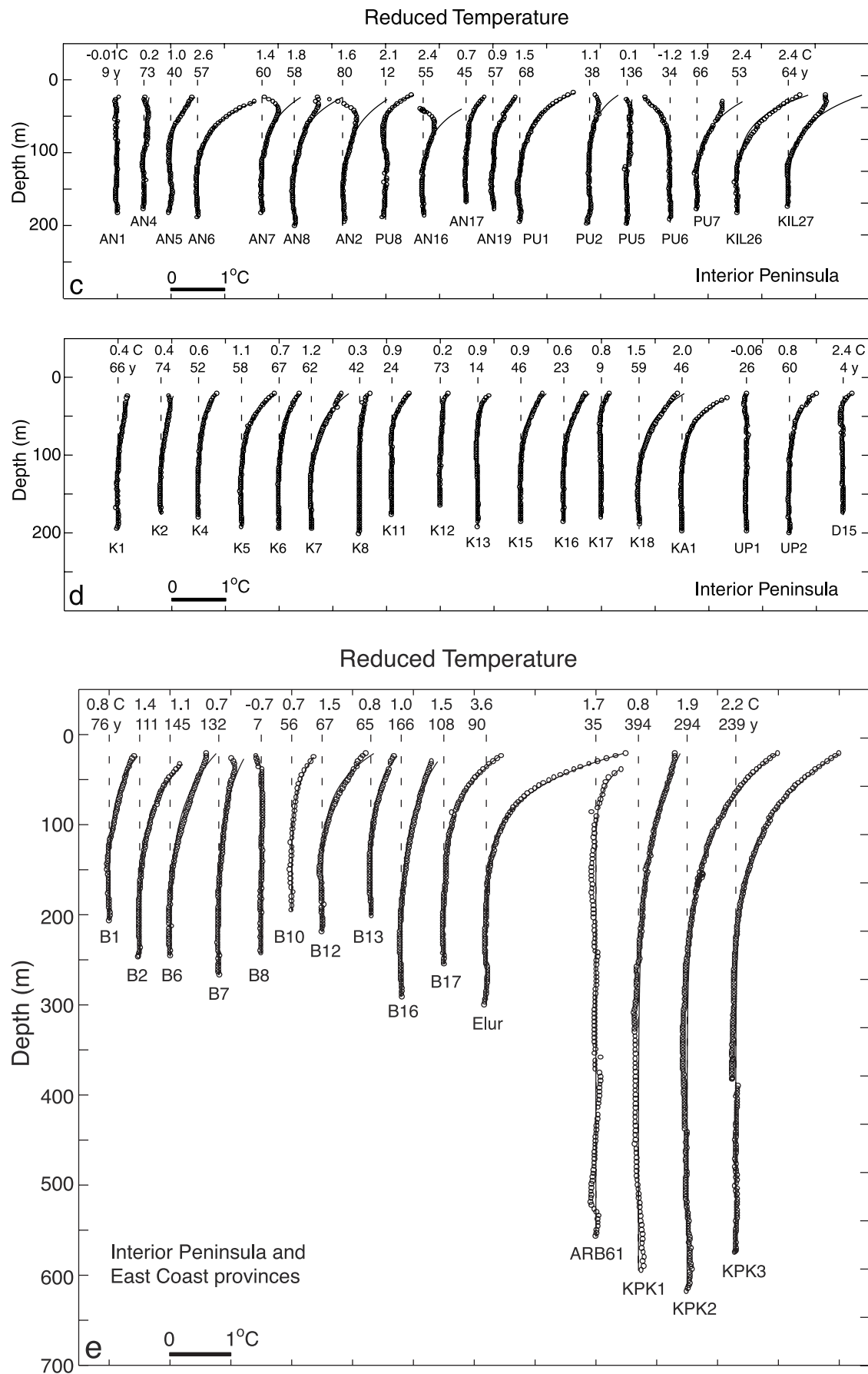
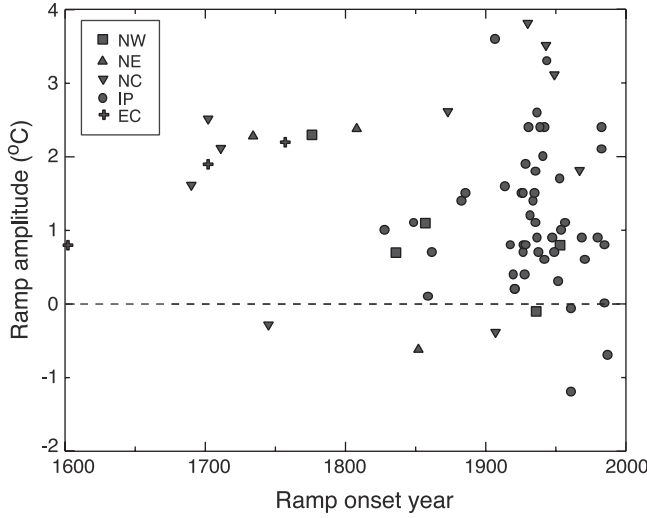


Figure 5. (continued)



**Figure 6.** Ramp amplitude and onset year for individual temperature profiles. Legend indicates climatic provinces of India: NW, northwest; NE, northeast; NC, north central; IP, interior peninsula; EC, east coast.

the reduced temperature profiles and provides a robust estimate of recent SGT change.

[18] Our model is parameterized in terms of a total warming (or cooling) magnitude  $\Delta T$  and a duration time  $t^*$  and can be expressed as [Carslaw and Jaeger, 1959; Lachenbruch and Marshall, 1986]

$$\Delta T(z) = 4\Delta T i^2 \operatorname{erfc}\left(\frac{z}{\sqrt{4\alpha t^*}}\right), \quad (3)$$

where  $i^2 \operatorname{erfc}$  is the second integral of the complimentary error function. A uniform thermal diffusivity of  $10^{-6} \text{ m}^2 \text{ s}^{-1}$  is assumed throughout the analysis. For other values of diffusivity the ramp duration  $t^*$  is easily adjusted by keeping the product  $(\alpha t^*)$  constant. To solve for the best fitting ramp function, we inverted equation (3) using a linearized Newton's method. Although our forward model operator is nonlinear with respect to  $t^*$ , we found that linearization of the operator provides an adequate approximation. This method is effective for nonlinear problems having few model parameters. Chisholm and Chapman [1992] employed a similar technique and investigated parameter resolution. They found that the ramp amplitude was much better resolved than the onset time. Furthermore, they found that if the ramp amplitude is increased while the onset time is decreased the root-mean-square (RMS) misfit slowly increases, relative to the case where both parameters are either increased or decreased. For our example borehole, Elur, the best fitting ramp amplitude is  $3.6^\circ\text{C}$ , and ramp duration is 90 years. We investigated how sensitive these parameters are with respect to the depth to the start of the linear fit,  $z^*$ . For  $z^*$  between 100 and 200 m the ramp amplitude does not vary from  $3.6^\circ\text{C}$  and the ramp duration varies between 60 and 90 years. This finding is consistent with the resolution results of Chisholm and Chapman [1992], indicating that the ramp amplitude is better resolved than the ramp duration.

[19] Model fits to the reduced temperature profiles (Figure 5) indicate good fits to most of the temperature profiles with an average RMS misfit of 30 mK. However, several temperature profiles in the IP (Figure 5c) are not well fit by a single ramp (AN7, AN8, AN2, AN16, PU2, PU7, and KIL27). These profiles indicate a more complex surface temperature history than can be fit with a simple trend and are discussed in section 4.2. A summary of individual ramp solutions (Table 2) for surface ground temperature change are plotted in Figure 6. Several points are worth noting. First, of the 70 boreholes, 63 (90%) indicate warming. Warming magnitudes vary between  $0^\circ$  and  $3.8^\circ\text{C}$  with a mean and standard deviation of  $1.3 \pm 1.0^\circ\text{C}$ . The onset time varies between 1985 and 1602 with a mean and standard deviation of  $1900 \pm 80$  years. Most warming signals in borehole records have onset times occurring between 1800 and 1960 A.D. Second, there is a large variability in the SGT solutions between the sites. This variability may result from one or more of the following factors: (1) our assumption of a bulk thermal conductivity throughout a borehole column and a uniform thermal diffusivity throughout the analysis; (2) site-specific perturbations in surface conditions such as vegetation cover, land use, and local microclimatic effects, and (3) boreholes are distributed over a large geographical region covering several climatic provinces. The first two of these factors can be considered noise, while the third factor may be reflecting something intrinsic to climatic change in India. We note that similar variability, ranging from  $-1.1$  to  $2.0^\circ\text{C}$ , is observed in warming magnitudes based on century-long trends estimated from 48 surface air temperature records considered in this study. Overall, the 70 profiles constitute a compelling new data set for investigating climate change on the Indian subcontinent.

#### 4.1. Regional Averages

[20] Several authors have pointed out that in the presence of regional SGT changes, an effective strategy for suppressing noise is to invert simultaneously for a common SGT

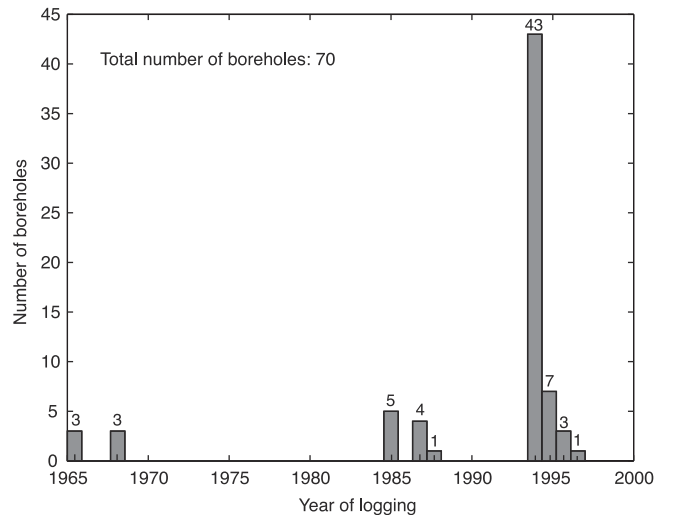


**Figure 7.** Histogram showing a distribution of the year of logging for the 70 boreholes selected for this study. A majority of the boreholes were logged during 1994–1995.

**Table 3.** Results of Simultaneous Inversion of Reduced Temperature Profiles<sup>a</sup>

Climatic Division	Number of Sites	Average $\Delta T$ , °C	Average $t^*$ , years	Average Trend, °C/100 years
All sites	70	0.86 (0.06)	149 (20)	0.58 (0.1)
Northwest (NW)	5	1.20 (0.23)	142 (49)	0.87 (0.34)
North central (NC)	10	1.61 (0.22)	158 (37)	1.02 (0.27)
Northeast (NE)	3	1.48 (0.31)	252 (110)	0.58 (0.28)
East coast (EC)	3	1.65 (0.09)	287 (33)	0.57 (0.1)
Interior peninsula (IP)	49	0.63 (0.06)	107 (16)	0.59 (0.1)

<sup>a</sup>  $\Delta T$ , ramp amplitude;  $t^*$ , ramp duration; numbers within parentheses indicate 95% confidence limits.

model [Clauser and Mareschal, 1995; Pollack et al., 1996; Beltrami et al., 1997]. Because the frequency content of the transient portion of temperature-depth profiles evolves with time, it is important to adjust boreholes that have been logged in different years. Figure 7 shows a histogram of the number of boreholes logged through time. Fortunately, most of the boreholes were logged between 1994 and 1996. However, six temperature logs in the NW and NE provinces were acquired between 1965 and 1968, five in the NC province were obtained in 1985, and another five in the IP were measured between 1987 and 1988. To account for these different logging dates, we have forward continued the temperature profiles to a common year 1994 [Harris and Chapman, 2001], by assuming a SGT rate of change between the year the borehole was logged and 1994 equal to the rate of SGT change determined from their respective ramp inversions. Ramp parameters determined from the original log and the forward continued log are similar indicating that this forward continuation process does not significantly change the results. It does, however, add to the consistency. Temperature profiles logged between 1994 and 1997 are left unchanged.

[21] A simultaneous ramp inversion of the 70 reduced temperature profiles indicate an average warming of  $0.9 \pm 0.1^\circ\text{C}$  over the past  $150 \pm 20$  years (Table 3) or a trend of  $0.6 \pm 0.1^\circ\text{C}/100$  years. These values are within the standard deviation of average ramp parameters reported in Table 2.

[22] To investigate possible regional climatic differences between these provinces, we have simultaneously inverted

the data for each climatic province (Table 3 and Figure 8). Simultaneous inversion of the reduced temperature profiles belonging to the IP province yields a tightly constrained value of  $\sim 0.6 \pm 0.1^\circ\text{C}$  over the past 107 years. The NC province has 10 boreholes all of which are distributed over a small area in the southern part of the province. The average SGT change for this province is estimated to be  $1.6^\circ\text{C}$  over the past 158 years. The averages for both the IP and NC provinces yield 100-year SGT warming trends that are consistent with those obtained from SAT data for the two provinces (Table 1). The other provinces have very limited spatial coverage by boreholes: all the boreholes in the NE and EC provinces are located at a single site in each province, and three out of five boreholes considered for analysis from the NW province belong to only one site. Therefore the SGT trends given in Table 3 for the NW, NE, and EC provinces may not be truly representative for these provinces. Additional coverage by boreholes may be necessary to constrain better the SGT history for these provinces. Overall, the available borehole

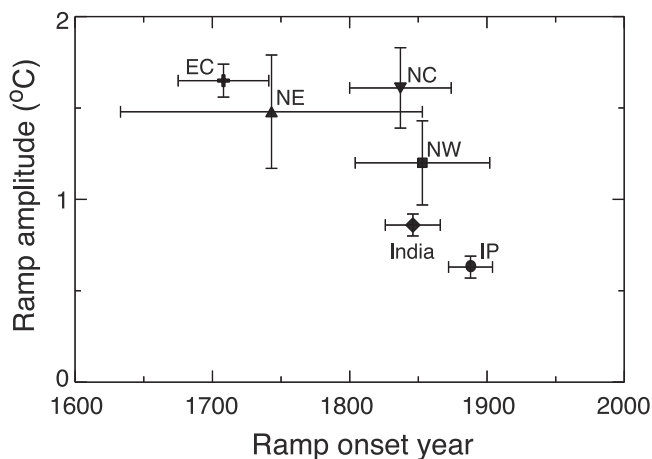


**Figure 8.** Results of simultaneous inversion of borehole reduced temperature profiles for ramp changes in SGT. Error bars represent 95% confidence limits for the ramp parameters. Symbols indicate climatic provinces shown in Figure 1.

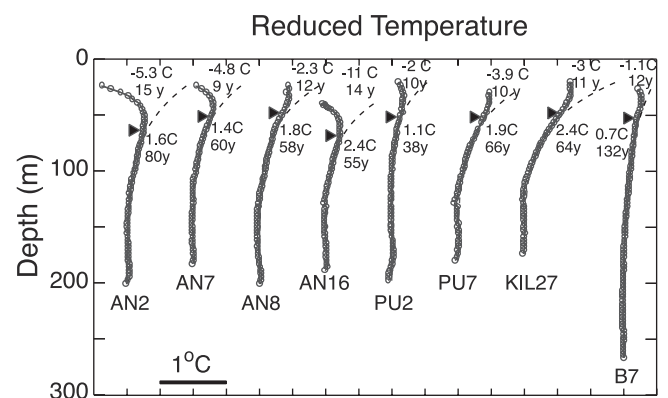


**Figure 9.** Reduced temperature profiles showing local evidence for cooling events of the last decade superimposed on the multidecadal regional warming events. The ramp fits to the regional warming signals at depth, which precede in time the recent cooling signatures observed in the shallow subsurface ( $<60$  m), are shown by dashed curves. These fits are obtained by inverting the transient temperatures below a depth  $Z_{\text{recent}}$  indicated by arrows. The parameters of these ramps are shown below the arrows and correspond to those given in Table 2. The “cooling anomalies” represented by departures of the reduced temperatures from the dashed curve in the upper part of the temperature profiles are modeled in terms of a second ramp of shorter duration. The parameters of the best fitting ramps are shown on top of each profile and are listed in Table 4.

**Table 4.** Events of the Last Two Decades, Summary of Ramp Inversion Results<sup>a</sup>

Location, Borehole	$Z_{\text{recent}}$ , m	$\Delta T$ , °C	$t^*$ , years	RMS, mK	Onset Year
Sidhatek, AN-2	63	−5.3	15	17	1979
Padli, AN-7	51	−4.8	9	11	1985
Taklibhan, AN-8	48	−2.3	12	25	1982
Brahmani, AN-16	69	−11.0	14	18	1980
Ambegaon, PU-2	51	−2.0	10	16	1985
Malwadi, PU-7	51	−3.9	10	15	1985
Petsangvi, KIL-27	48	−3.0	11	20	1984
Vijayapura, B-7	51	−1.1	12	14	1982

<sup>a</sup> $Z_{\text{recent}}$  is depth below which a ramp model simulating an increase in surface ground temperature is fit to the reduced temperature profile. The departures of this ramp model (described in Table 2) from the reduced temperature profile are then modeled in terms of another ramp function, the parameters ( $\Delta T$  and  $t^*$ ) of which are listed here. RMS refers to the root-mean-square misfit corresponding to the second ramp fit.

temperature data do not indicate any significant spatial variation pattern in the SGT histories over India.

#### 4.2. Events of the Last Decade

[23] While most reduced temperature profiles show a monotonic trend of either increasing or decreasing reduced temperature that are well fit by a ramp function, some temperature logs exhibit a more complex pattern of reduced temperature. *Lachenbruch and Marshall* [1986] observed similar patterns for some Alaska sites and related the changes to modifications of surface conditions produced by construction of drilling pads. We found eight borehole temperature profiles which could not be fit adequately with a single ramp model, particularly in the upper  $\sim 50$ – $60$  m. These anomalous profiles correspond to the boreholes AN2, AN7, AN8, AN16, PU2, PU7, KIL27, and B7. These sites are all located within the IP province, and all indicate a recent cooling signal superimposed on a longer warming trend.

[24] We analyze the recent cooling signals in each of these boreholes by first fitting the reduced temperature profile with a ramp increase of surface temperature below the depth  $Z_{\text{recent}}$  (Figure 9). These solutions correspond to the ramp parameters listed in Table 2. These ramp fits are shown as dashed curves, extended above  $Z_{\text{recent}}$  based on the model parameters of the respective ramps. These extended dashed curves represent estimates of what the temperature profiles might have been in the absence of the recent cooling. We consider  $Z_{\text{recent}}$  to be an indicator of the estimated depth limit of penetration of the most recent cooling event. The “cooling” anomalies at each depth, i.e., the differences between the dashed curve and the reduced temperatures for a borehole, are then fit with a second ramp as shown by the solid lines in Figure 9. In general, the analysis reveals a variable,  $\sim 1$ – $5^\circ\text{C}$  cooling, relative to the continued earlier warming ramp, over a brief duration of 9–15 years corresponding to an onset time of 1979–1985 (Table 4). Because these boreholes have several other boreholes in their immediate vicinity which do not exhibit such “recent cooling” signatures, we tentatively attribute these features to site-specific ground surface perturbations possibly resulting from changes in local land use.

#### 5. Joint Analysis of Borehole and Meteorological Data

[25] The results of our borehole temperature analysis indicate regional SGT warming of  $0.9^\circ\text{C}$  over the past 150 years. This corresponds well with a warming trend of

$0.5^\circ\text{C}/100$  years determined from nearby meteorological stations and suggests that ground and air temperature changes track each other. We now formally compare the borehole and SAT data. However, because of differences in the frequency and temporal content between the signal of surface warming contained in SAT records and borehole temperatures, the two data sets cannot be readily compared (see *Harris and Chapman* [1998b] for a detailed discussion). The Earth is a low-pass filter such that the high-frequency signal associated with SGT change is progressively filtered out with depth. In contrast, SAT time series represent discrete measurements made at specific times with annual resolution. One method for comparing these two signals is to filter the SAT data by computing a synthetic temperature-depth profile. The process essentially filters the SAT data so that they have similar frequency content to the reduced temperature profiles. Studies by *Lachenbruch et al.* [1988], *Harris and Chapman* [1997], and *Harris and Gosnold* [1999] have shown that synthetic temperature profiles computed from SAT records at nearby meteorological stations reproduce inferred borehole temperature transients. Further, these studies suggest that borehole transient temperature profiles have the potential to yield long-term trends in surface ground temperature.

[26] For identifying regional climatic trends in the data we compare the borehole reduced temperature profiles for each province with the average synthetic transient profile constructed using the average SAT time series. Again boreholes logged prior to 1994 are forward continued to 1994.

[27] A synthetic transient temperature-depth profile,  $T_{\text{RSAT}}(z)$ , is computed from a SAT time series by expressing the SAT record as a sequence of  $N$  individual step functions of amplitude  $\Delta T_i$  and time prior to the borehole temperature measurement  $\tau_i$  [*Carslaw and Jaeger*, 1959],

$$T_{\text{RSAT}}(z) = \sum_{i=1}^N \Delta T_i \text{erfc}\left(\frac{z}{\sqrt{4\alpha\tau_i}}\right), \quad (4)$$

where  $\text{erfc}$  is the complementary error function and  $\alpha$  is the thermal diffusivity. The first step change in temperature,  $\Delta T_1$ , can be expressed as  $\Delta T_1 = (\text{POM} - T_1)$ , where POM is the preobservational mean temperature and represents a weighted average of surface temperatures prior to the advent of the SAT records at  $\tau_1$  [*Harris and Chapman*, 1997]. The POM is determined by finding an initial temperature that minimizes the misfit between the synthetic transient temperatures generated from the SAT data and the borehole



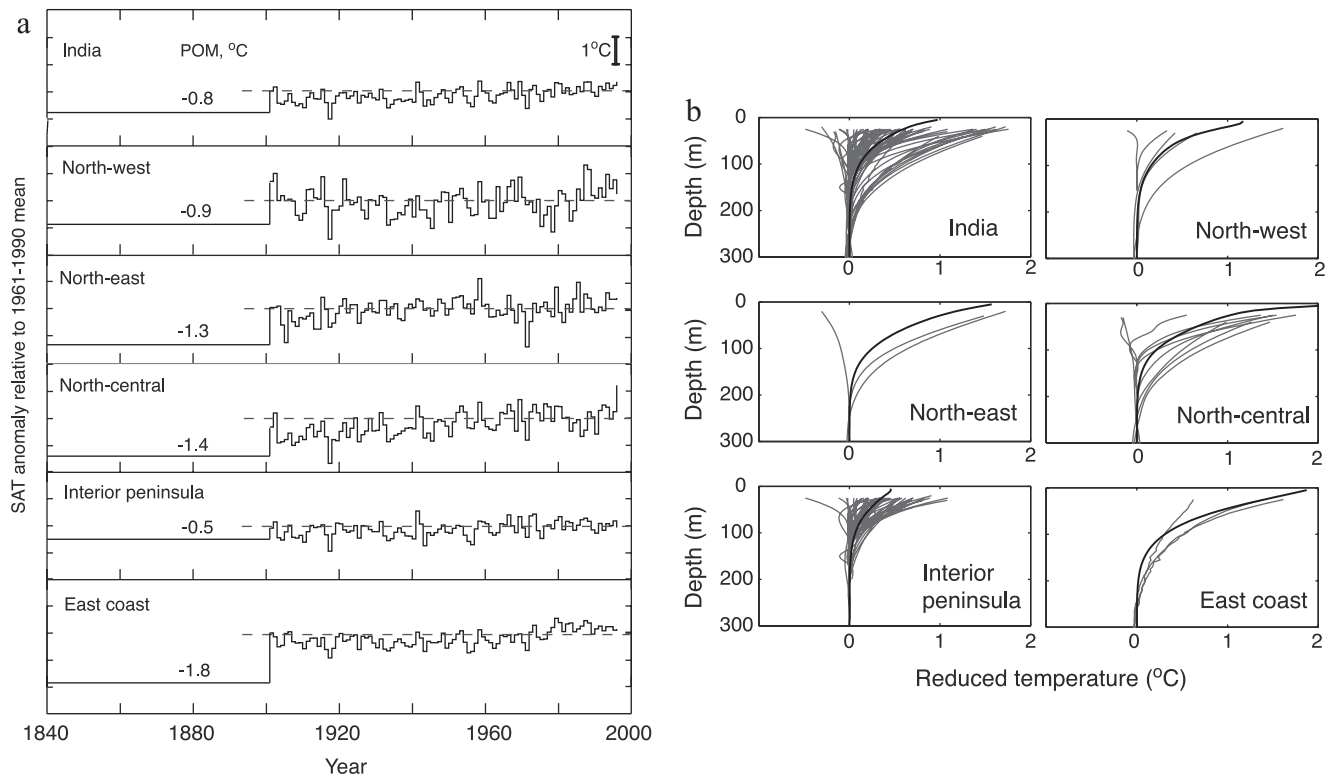


**Figure 10.** Combining borehole transient temperature and SAT data for India. (a) Preobservational mean (POM) temperatures relative to the 1961–1990 mean SATs (dashed lines) are shown along with average SAT time series (staircase plots) for the respective climatic provinces. (b) Computed reduced temperature profiles (thick lines) corresponding to the best fitting POM-SAT combinations shown in Figure 10a along with borehole reduced temperature profiles (thin lines) for all sites in the different provinces.

reduced temperatures with an arbitrary constant offset. *Harris and Chapman* [1997, 1998b] have demonstrated the robustness of such a comparison. The POM is expressed relative to the 1961–1990 mean SAT.

[28] A joint analysis of borehole and SAT data is carried out for all of India and separately for the five climatic provinces. The best fitting POM temperatures are listed in Table 5. POM-SAT models and synthetic temperature profiles produced by these models are shown in Figure 10. When all borehole and SAT records are considered, the best fitting POM corresponds to a temperature  $0.8 \pm 0.1^\circ\text{C}$  lower than the 1961–1990 mean SAT for all India. This estimate for POM temperature compares favorably with the recent estimate of  $0.7^\circ\text{C}$  for the Northern Hemisphere midlatitude region from similar studies [*Harris and Chapman*, 2001]. The best fitting POM-SAT model for data from the Interior peninsula results in a POM of  $0.5^\circ\text{C}$  cooler than the 1961–1990 mean SAT. However, for other climatic provinces the best fitting POM-SAT models yield relatively larger values for POM between  $0.9$  and  $1.8^\circ\text{C}$  cooler than the 1961–1990 mean SAT. The POMs for all the provinces are significantly lower than the corresponding 1961–1990 mean SATs, suggesting that the warming trends observed in the SAT records represent significant increases from the preinstrumental (19th century) conditions.

[29] Availability of annual meteorological data for the most recent decade permit an analysis of total warming from

the baseline temperature in the early 1800s to the present day. The 1990s have been warm in India, as for most of the globe. Relative to the 1961–1990 mean temperature, SAT averages for India from 1995 through 1999 are  $0.32$ ,  $0.10$ ,  $0.31$ ,  $0.92$ , and  $0.37^\circ\text{C}$ , respectively, or  $0.40^\circ\text{C}$  on average [*Jones et al.*, 2001]. Thus the total surface warming in India from the early 1800s to the late 1900s is  $\sim 1.2^\circ\text{C}$ .

## 6. Summary

[30] Analysis of an extensive set of borehole temperature profiles and meteorological data spatially distributed over a large region in India and covering five climatic provinces leads to the following conclusions.

**Table 5.** Results of Joint Analysis of Geothermal and Meteorological Data<sup>a</sup>

Region	POM, $^\circ\text{C}$	RMS, $^\circ\text{C}$
India (all sites)	−0.8	0.23
Northwest province	−0.9	0.26
Northeast province	−1.3	0.40
North central province	−1.4	0.30
Interior peninsula	−0.5	0.19
East coast	−1.8	0.18

<sup>a</sup>POM is the best fitting preobservational mean relative to the 1961–1990 mean SAT; RMS is the root-mean-square of the model fit to the borehole transient temperature profiles for each group.

1. Last event “ramp” analyses of 70 borehole temperature-depth profiles reveal an average surface ground warming of  $\sim 0.9 \pm 0.1^\circ\text{C}$  over the past  $\sim 150$  years. The majority of the warming amplitudes ranges from 0.4 to  $2.6^\circ\text{C}$  and indicate onset times between 1800 and 1960.

2. Surface air temperature (SAT) data distributed over a comparable region indicate an average rate of warming of  $0.5^\circ\text{C}/100$  years, similar to that revealed by borehole temperature profiles. Borehole temperatures indicate that in many areas, warming began before widespread recording of SAT data in India.

3. Joint analysis using data from all borehole and meteorological stations used in this study yields a best fitting POM-SAT model with a long-term preobservational mean (POM) temperature  $0.8^\circ\text{C}$  lower than the 1961–1990 mean SAT. Total warming between a circa 1800 baseline and the late 1990s appears to be  $\sim 1.2^\circ\text{C}$ .

[31] **Acknowledgments.** We appreciate efforts made by National Geophysical Research Institute (NGRI) for sustained borehole temperature data acquisition over the past 35 years, without which the past climate change signals could not have been unearthed. The surface air temperature data was obtained from the National Data Center of the India Meteorological Department, Pune. The work was started during the tenure of a research fellowship provided to S.R. by Council of Scientific and Industrial Research, India, at NGRI and completed during the tenure of BOYSCAST fellowship awarded to S.R. by the Department of Science and Technology, Government of India tenable at the University of Utah, Salt Lake City. S.R. has benefited from the IGCP 428 program during the 1999 IUGG General Assembly held at Birmingham, UK. We thank H. Beltrami and an anonymous reviewer for constructive and helpful reviews. We thank K. Sain for help with an inversion algorithm during the early part of the work and M. Bartlett and P. Gettings at several stages of the work. The paper has benefited from discussions with A. H. Lachenbruch, H. N. Pollack, and S. Huang. We are grateful to Harsh K Gupta for support and sustained encouragement and S. M. Naqvi, Director, NGRI for permission to publish the paper.

## References

- Beck, A. E., and A. Judge, Analysis of heat flow data, I, Detailed observations in a single borehole, *Geophys. J. R. Astron. Soc.*, **18**, 145–158, 1969.
- Beltrami, H., and D. S. Chapman, Drilling for a past climate, *New Sci.*, **1922**, 36–40, 1994.
- Beltrami, H., L. Cheng, and J. C. Mareschal, Simultaneous inversion of borehole temperature data for determination of ground surface temperature history, *Geophys. J. Int.*, **129**, 311–318, 1997.
- Blackwell, D. D., J. L. Steele, and C. A. Brott, The terrain effect on terrestrial heat flow, *J. Geophys. Res.*, **85**, 4757–4772, 1980.
- Carslaw, H. S., J. C. Jaeger, *Conduction of Heat in Solids*, 2nd ed., 386 pp. Oxford Univ. Press, New York, 1959.
- Cermak, V., L. Bodri, and J. Safanda, Recent climatic change recorded in the underground: Evidence from Cuba, *Palaeogeogr. Palaeoclimatol. Palaeoecol.*, **98**, 219–224, 1992.
- Chapman, D. S., T. J. Chisholm, and R. N. Harris, Combining borehole temperature and meteorologic data to constrain past climate change, *Palaeogeogr. Palaeoclimatol. Palaeoecol.*, **98**, 269–281, 1992.
- Chisholm, T. J., and D. S. Chapman, Climate change inferred from analysis of borehole temperatures: An example from western Utah, *J. Geophys. Res.*, **97**, 14,155–14,175, 1992.
- Clauser, C., and J.-C. Mareschal, Ground temperature history in central Europe from borehole temperature data, *Geophys. J. Int.*, **121**, 805–817, 1995.
- Clow, G. D., The extent of temporal smearing in surface-temperature histories derived from borehole temperature measurements, *Palaeogeogr. Palaeoclimatol. Palaeoecol.*, **98**, 81–86, 1992.
- Crowley, T. J., and T. S. Lowery, How warm was the Medieval warm period?, *Ambio*, **29**, 51–54, 2000.
- Deming, D., Evidence for climatic warming in North America from analysis of borehole temperatures, *Science*, **268**, 1576–1577, 1995.
- Ellsaesser, H. W., M. C. MacCracken, J. J. Walton, and S. L. Grotch, Global climatic trends as revealed by the recorded data, *Rev. Geophys.*, **24**, 745–792, 1986.
- Guillou-Frottier, L., J.-C. Mareschal, and J. Musset, Ground surface temperature history in central Canada inferred from 10 selected borehole temperature profiles, *J. Geophys. Res.*, **103**, 7385–7397, 1998.
- Gupta, M. L., Thermal regime of the Indian shield, in *Terrestrial Heat Flow and Geothermal Energy in Asia*, edited by M. L. Gupta and M. Yamano, pp. 63–81, Oxford and IBH, New Delhi, 1995.
- Gupta, M. L., R. K. Verma, R. U. M. Rao, V. M. Hamza, and G. V. Rao, Terrestrial heat flow in the Khetri copper belt, Rajasthan, India, *J. Geophys. Res.*, **72**, 4215–4220, 1967.
- Gupta, M. L., S. R. Sharma, and A. Sundar, Heat flow and heat generation in the Archaean Dharwar cratons and implications for the southern Indian Shield geotherm and lithospheric thickness, *Tectonophysics*, **194**, 107–122, 1991.
- Gupta, M. L., A. Sundar, S. R. Sharma, and S. B. Singh, Heat flow in the Bastar Craton, central Indian shield: Implications for thermal characteristics of Proterozoic cratons, *Phys. Earth Planet. Inter.*, **78**, 23–31, 1993.
- Hansen, J., and S. Lebedeff, Global trends of measured surface air temperatures, *J. Geophys. Res.*, **92**, 13,345–13,372, 1987.
- Harris, R. N., and D. S. Chapman, Climate change on the Colorado Plateau of eastern Utah inferred from temperatures, *J. Geophys. Res.*, **100**, 6367–6381, 1995.
- Harris, R. N., and D. S. Chapman, Borehole temperatures and a baseline for 20th-century global warming estimates, *Science*, **275**, 1618–1621, 1997.
- Harris, R. N., and D. S. Chapman, Geothermics and climate change, 1, Analysis of borehole temperatures with emphasis on resolving power, *J. Geophys. Res.*, **103**, 7363–7370, 1998a.
- Harris, R. N., and D. S. Chapman, Geothermics and climate change, 2, Joint analysis of borehole temperatures and meteorological data, *J. Geophys. Res.*, **103**, 7371–7383, 1998b.
- Harris, R. N., and D. S. Chapman, Mid-latitude ( $30^\circ$ – $60^\circ\text{N}$ ) climatic warming inferred by combining borehole temperatures with surface air temperatures, *Geophys. Res. Lett.*, **28**, 747–750, 2001.
- Harris, R. N., and W. D. Gosnold, Comparisons of borehole temperature-depth profiles and surface air temperatures in the northern plains of the USA, *Geophys. J. Int.*, **138**, 541–548, 1999.
- Hingane, L. S., K. Rupakumar, and B. V. Ramamurthy, Long term trends of surface air temperature in India, *J. Climatol.*, **5**, 521–528, 1985.
- Huang, S., H. N. Pollack, and P. Y. Shen, Temperature trends over the past five centuries reconstructed from borehole temperatures, *Nature*, **403**, 756–758, 2000.
- Jaeger, J. C., The effect of the drilling fluid on temperatures measured in boreholes, *J. Geophys. Res.*, **66**, 563–569, 1961.
- Jagannathan, P., and B. Parthasarathy, Fluctuations in the seasonal oscillation of temperature in India, *Indian J. Meteorol. Geophys.*, **23**, 15–22, 1972.
- Jones, P. D., K. R. Briffa, T. P. Barnett, and F. B. S. Tett, High-resolution palaeoclimatic records for the last millennium, *Holocene*, **8**, 455–471, 1998.
- Jones, P. D., M. New, D. E. Parker, S. Martin, and I. G. Rigor, Surface air temperature and its changes over the past 150 years, *Rev. Geophys.*, **37**, 173–199, 1999.
- Jones, P. D., T. J. Osborn, K. R. Briffa, C. K. Folland, E. B. Horton, L. V. Alexander, D. E. Parker, and N. A. Rayner, Adjusting for sampling density in grid box land and ocean surface temperature time series, *J. Geophys. Res.*, **106**, 3371–3380, 2001.
- Lachenbruch, A. H., and B. V. Marshall, Changing climate: Geothermal evidence from permafrost in the Alaskan Arctic, *Science*, **234**, 689–696, 1986.
- Lachenbruch, A. H., T. T. Cladouhos, R. W. Saltus, Permafrost temperature and the changing climate, in *Proceedings of the 5th International Conference on Permafrost*, pp. 1535–1543, Tapir, Trondheim, 1988.
- Lewis, T. J., and K. Wang, Influence of terrain on bedrock temperatures, *Palaeogeogr. Palaeoclimatol. Palaeoecol.*, **98**, 87–100, 1992.
- Mann, M. E., R. S. Bradley, and M. K. Hughes, Global-scale temperature patterns and climate forcing over the past six centuries, *Nature*, **392**, 779–787, 1998.
- Mann, M. E., R. S. Bradley, and M. K. Hughes, Northern Hemisphere temperatures during the past millennium: Inferences, uncertainties and limitations, *Geophys. Res. Lett.*, **26**, 759–762, 1999.
- Mareschal, J. C., and H. Beltrami, Evidence for recent warming from perturbed geothermal gradients: Examples from eastern Canada, *Clim. Dyn.*, **6**, 135–143, 1992.
- Overpeck, J., et al., Arctic environmental change of the last four centuries, *Science*, **278**, 1251–1256, 1997.
- Pollack, H. N., P. Y. Shen, and S. Huang, Inference of ground surface temperature history from subsurface temperature data: Interpreting ensembles of borehole logs, *Pure Appl. Geophys.*, **147**, 537–550, 1996.
- Pollack, H. N., S. Huang, and P. Y. Shen, Climate change revealed by subsurface temperatures: A global perspective, *Science*, **282**, 279–281, 1998.

- Pramanik, S. K., and P. Jagannathan, Climatic changes in India, II Temperature, *Indian J. Meteorol. Geophys.*, 5, 29–47, 1954.
- Rao, R. U. M., and G. V. Rao, Results of some geothermal studies in Singbhum thrust belt, India, *Geothermics*, 3, 153–161, 1974.
- Roy, R. F., D. D. Blackwell, E. R. Decker, Continental heat flow, in *The Nature of the Solid Earth*, pp. 506–543, McGraw-Hill, New York, 1972.
- Roy, S., and R. U. M. Rao, Geothermal investigations in the 1993 Latur earthquake area, Deccan Volcanic Province, India, *Tectonophysics*, 306, 237–252, 1999.
- Roy, S., and R. U. M. Rao, Heat flow in the Indian shield, *J. Geophys. Res.*, 105, 25,587–25,604, 2000.
- Rupa Kumar, K., and L. S. Hingane, Long-term variations of surface air temperature at major industrial cities of India, *Clim. Change*, 13, 287–307, 1988.
- Rupa Kumar, K., K. Krishna Kumar, and G. B. Pant, Diurnal asymmetry of surface temperature trends over India, *Geophys. Res. Lett.*, 21, 677–680, 1994.
- Sarker, R. P., and V. Thapliyal, Climate change and variability, *Mausam*, 39, 127–138, 1988.
- Shen, P. Y., and A. E. Beck, Least squares inversion of borehole temperature measurements in functional space, *J. Geophys. Res.*, 96, 19,965–19,979, 1991.
- Shen, P. Y., and A. E. Beck, Palaeoclimate change and heat flow density inferred from temperature data in the Superior Province of the Canadian Shield, *Global Planet. Change*, 6, 143–165, 1992.
- Srivastava, H. N., B. N. Dewan, S. K. Dikshit, G. S. Prakash Rao, S. S. Singh, and K. R. Rao, Decadal trends in climate over India, *Mausam*, 43, 7–20, 1992.
- Thapliyal, V., Perspective of climate change in India, *Report of the Expert Meeting on Climate Change Detection Project, Toronto, Niagara-on-the-Lake*, 26–30 Nov., World Meteorol.Org., Geneva, 1990.
- Thapliyal, V., and S. M. Kulshrestha, Climate changes and trends over India, *Mausam*, 42, 333–338, 1991.
- Wang, K., Estimation of ground surface temperatures from borehole temperature data, *J. Geophys. Res.*, 97, 2095–2106, 1992.

---

D. S. Chapman and R. N. Harris, Department of Geology and Geophysics, University of Utah, 135 S 1460 E, Room 719, Salt Lake City, UT 84112-0111, USA. (dchapman@park.admin.utah.edu)

R. U. M. Rao and S. Roy, National Geophysical Research Institute, P.O. Bag 724, Hyderabad, AP 500-007, India.